

Data driven structure property relationship and rational design of rare-earth magnetostrictive materials

Dan Liu(刘丹), Ying Tong(童颖), Yuan Li(李渊), Xinqi Zheng(郑新奇), Qiong Wu(吴琼), Ruoshui Liu(刘若水), Xin Ming(明昕), Yinong Yin(尹亦农), Jianfeng Xi(息剑峰), Tongyun Zhao(赵同云), Fengxia Hu(胡凤霞), Baogen Shen(沈保根)

Citation: Chin. Phys. B. 35, 097505 (2026). DOI: 10.1088/1674-1056/ae9a57 |
CSTR: 32038.14.CPB.ae9a57
http://cpb.iphy.ac.cn; http://iopscience.iop.org/cpb

What follows is a list of articles you may be interested in

Enhancement of cutoff frequency for planar anisotropic Y2Co17 by reductive diffusion method

Qianyang Zhou(周钱阳), Kai Long(龙凯), Rongfang Zhang(张榕芳), Baorui Xia(夏宝瑞)
Chin. Phys. B. 35, 087502 (2026). DOI: 10.1088/1674-1056/ae3064 | CSTR: 32038.14.CPB.ae3064

Review of the strategies for regulating working temperatures of rare-earth-based low temperature magnetic cooling materials

Jie Zhao(赵洁), Yawei Gao(高亚伟), Dingsong Wang(王鼎淞), Shuxian Yang(杨淑娴), Lei Xi(奚磊), Hao Liu(刘昊), Yang Pan(潘洋), Jiawang Xu(许家旺), Xinqi Zheng(郑新奇), Shouguo Wang(王守国)
Chin. Phys. B. 35, 077501 (2026). DOI: 10.1088/1674-1056/ae3f92 | CSTR: 32038.14.CPB.ae3f92

Magnon polarons: Hybrid quasiparticles in coupled spin–lattice systems

Yufei Li(李宇飞), Qi Gu(古琪), Mingzhi Wang(王铭志), Jia-Min Lai(来嘉敏), Aizhuo Zhang(张爱茁), Yameng Guo(郭雅萌), Yuhao Xia(夏宇浩), Yaowen Liu(刘要稳), Jianwei Zhang(张建卫), Wei Zhang(张伟), Zhiyong Quan(全志勇), Zhong Shi(时钟), Xiaohong Xu(许小红)
Chin. Phys. B. 35, 047507 (2026). DOI: 10.1088/1674-1056/ae5efc | CSTR: 32038.14.CPB.ae5efc

One-step synthesis of ThMn12-type Sm0.8Zr0.2Fe11SiBx (x = 0–0.2) ribbon magnets via rapid solidification

Chi Zhang(张驰), Hui-Dong Qian(千辉东), Wenyun Yang(杨文云), Jingzhi Han(韩景智), Xuegang Chen(陈学刚), Jinbo Yang(杨金波)
Chin. Phys. B. 34, 077501 (2025). DOI: 10.1088/1674-1056/add006 | CSTR: 32038.14.CPB.add006

Insights into the regulation mechanism of ring-shaped magnetoelectric energy harvesters via mechanical and magnetic conditions

Yang Shi(师阳), Ni Li(李妮), Yong Yang(杨勇)
Chin. Phys. B. 30, 107503 (2021). DOI: 10.1088/1674-1056/abeee9

TOPICAL REVIEW — AI + Physical Science

Data driven structure property relationship and rational design of rare-earth magnetostrictive materials

Dan Liu(刘丹)[1,†], Ying Tong(童颖)[1], Yuan Li(李渊)[1], Xinqi Zheng(郑新奇)[2], Qiong Wu(吴琼)[3], Ruoshui Liu(刘若水)[4], Xin Ming(明昕)[4], Yinong Yin(尹亦农)[1], Jianfeng Xi(息剑峰)[1,‡], Tongyun Zhao(赵同云)[5], Fengxia Hu(胡凤霞)[5], and Baogen Shen(沈保根)[4,5,§]

[1] *Department of Physics, Beijing Technology and Business University, Beijing* 100048, *China*
[2] *School of Materials Science and Engineering, University of Science and Technology Beijing, Beijing* 100083, *China*
[3] *School of Materials Science and Engineering, Beijing University of Technology, Beijing* 100124, *China*
[4] *Feicui Lake Laboratory, School of Materials Science and Engineering, Anhui University, Hefei* 230601, *China*
[5] *State Key Laboratory of Magnetism, Institute of Physics, Chinese Academy of Sciences, Beijing* 100190, *China*

(Received 24 April 2026; revised manuscript received 11 August 2026; accepted manuscript online 17 August 2026)

Rare-earth magnetostrictive materials possess irreplaceable strategic value in fields such as national defense, precision actuation, and smart sensing. Conventional materials development relies heavily on experimental trial-and-error approaches, first-principles calculations, and numerical simulations. However, owing to the complexity of multiphysics coupling, weak cross-scale correlations, and high computational cost, it is difficult to achieve both high efficiency and high accuracy. This paper systematically reviews recent progress in the application of machine learning (ML) to rare-earth magnetostrictive materials. From electronic structure and microstructural evolution to macroscopic property responses, the review clarifies the physical information transmission pathways between different scales. Furthermore, the challenges and development opportunities faced by cross-scale information fusion for machine learning-assisted design of magnetostrictive materials are discussed. ML methods are then classified and summarized according to different research scenarios, including property prediction, composition optimization, structure–property mapping, and parameter design for rare-earth magnetostrictive materials. In addition, this review further analyzes several core issues currently faced in this field and provides an outlook on future developments. This review provides a reference for the integration of data-driven methods and physical mechanisms, as well as for the design of high-performance magnetostrictive materials.

Keywords: magnetostrictive materials, rare earth, machine learning, physically interpretable framework, Fe-based alloys

PACS: 75.80.+q, 71.20.Eh, 07.05.Mh, 75.50.−y

DOI: 10.1088/1674-1056/ae9a57 **CSTR:** 32038.14.CPB.ae9a57

1. Introduction

Magnetostrictive materials represent a class of functional materials characterized by their ability to undergo macroscopic dimensional variations under an applied magnetic field, or conversely, to exhibit modulations in magnetization state when subjected to external mechanical stress.[1–3] The magnetostrictive effect in these materials stems from the synergistic interplay of physical mechanisms across multiple length scales. At the microscopic scale, the reorientation of electron spins induces minute lattice distortions mediated by spin–orbit coupling. Macroscopically, the cumulative effect of these distortions, combined with the irreversible motion of magnetic domain walls, manifests as significant dimensional changes in the bulk material. Based on the magnitude of the magnetostrictive response and its thermal stability, these materials are generally categorized into traditional magnetostrictive alloys and rare-earth giant magnetostrictive materials.

Rare-earth giant magnetostrictive materials (GMMs) are exemplified by rare-earth–iron intermetallic compounds like Terfenol-D. These materials occupy a pivotal strategic position in both defense and civilian sectors. Their applications range from sonar detection to precision actuation and intelligent vibration damping. Their indispensability stems from an exceptional combination of giant magnetostriction (λ) and high energy densities. They also exhibit rapid response characteristics.[4] In contrast, iron-based magnetostrictive alloys consist predominantly of the Fe–Ga binary system. These alloys have garnered extensive utility in sensors, medical instrumentation, and actuator applications. They are distinguished from traditional counterparts by superior magnetostriction coefficients. Furthermore, they possess robust mechanical integrity and elevated Curie temperature (T_c). Nevertheless, conventional material discovery relies on empirical

†Corresponding author. E-mail: liudan@btbu.edu.cn
‡Corresponding author. E-mail: xijf@btbu.edu.cn
§Corresponding author. E-mail: shenbg@iphy.ac.cn

© 2026 Chinese Physical Society and IOP Publishing Ltd. All rights, including for text and data mining, AI training, and similar technologies, are reserved.

trial-and-error and standard computational simulations. These methods remain constrained by the intrinsic complexity of the material systems. Consequently, efficient and cost-effective exploration proves difficult. From an experimental standpoint, performance is strongly influenced by composition and processing conditions. The intricate interplay of multicomponent synergies critically dictates microstructural evolution. Moreover, interfacial reactions directly influence macroscopic magnetostrictive behavior. Therefore, systematic experimental screening is often required to optimize composition and processing conditions. This process necessitates prolonged cycles and complex operations. It also incurs prohibitive costs due to the consumption of precious metals and rare resources. From a computational perspective, challenges remain equally pronounced. First-principles methods based on density functional theory effectively elucidate atomic-scale electronic structures. However, their high computational cost restricts applicability to high-throughput screening. This is particularly true for complex or multicomponent systems. Conversely, mesoscopic methods such as molecular dynamics can address larger scales. Yet, they fail to rigorously bridge the gap between atomic-level mechanisms and macroscopic properties. This disconnect limits the predictive efficacy of current models. Ultimately, it exacerbates the inefficiency of research and development.

The deep integration of ML techniques with materials informatics offers a transformative paradigm to overcome current research and experimental development bottlenecks.[5–7] Agada *et al.*[8] propose a hybrid ML framework combining physically-constrained variational autoencoder and Bayesian optimization to speed up crystal-structure refinement with defects. This method applies to complex materials for exploring structure-property relations. It offers a new idea of combining crystallography and ML for magnetic-material study. Similarly, Wei *et al.*[9] predicted the high-temperature oxidation and corrosion behavior of GMMs. Consequently, they achieved optimized durability and stability. Moreover, ML can precisely modulate the microstructure of structure-sensitive rare-earth materials. It achieves this by identifying optimal processing windows. For instance, Jie *et al.*[10] focused on low-cost Nd–Fe–B magnets. They utilized an adaptive learning loop integrating random forest (RF) and Gaussian process regression. This approach simultaneously optimized chemical composition and heat treatment protocols. This methodology successfully screened for optimal combinations within a multidimensional parameter space. It pinpointed the ideal annealing temperature window for specific compositions. Thus, it effectively balanced coercivity (H_c) against production costs. ML leverages statistical algorithms to mine latent structure–property relationships from vast datasets. This capability enables rapid performance prediction and virtual screening of novel materials. Additionally, it facilitates the intelligent optimization of processing parameters.

2. Method

According to task types, ML can be divided into regression tasks, classification tasks, clustering tasks, and generation tasks. For magnetostrictive materials, the prediction of continuous numerical values such as λ, T_c, saturation magnetization (M_s), and H_c all belong to regression tasks. Table 1 lists the ML models suitable for such regression tasks, together with their advantages and disadvantages.

Table 1. Advantages and disadvantages of commonly used machine learning algorithms.

Model	Advantage	Disadvantage
ANN	Strong generalization capability and support for multiple input and output variables	Prone to overfitting, complex hyperparameter tuning
ELM	Fast training speed and strong generalization ability, less prone to overfitting	Sensitive to noisy data and has poor interpretability
CNNs	No manual feature engineering required, with strong generalization capability	High computational complexity and complex network structure
DTR	Intuitive and interpretable, handles nonlinear relationships	Prone to overfitting, weak generalization ability, and sensitivity to noise data
RF	Strong generalization ability and output feature importance	High computational complexity; poor performance on small sample data
GBDT	High prediction accuracy, suitable for small samples and high-dimensional data	Training is slow, sensitive to parameters, and prone to overfitting
SVR	Strong generalization ability under small sample size and handling nonlinear data	High computational complexity and parameter sensitivity
KNN	No training process required. Simple implementation and no explicit model-training phase.	The full-sample distance must be calculated, which is highly affected by the dimensionality curse.

2.1. Model based on neural network

Neural network models mimic biological brain structures. They handle complex non-linear relationships and excel at tasks such as classification, regression, and pattern recognition.[11] Artificial neural networks (ANNs) constitute a pivotal branch of ML. They consist of interconnected neurons organized into input, hidden, and output layers.[12] In magnetostrictive material research, ANNs accurately predict performance by learning complex relationships among composition, processing, and properties. They possess strong generalization capabilities and handle high-dimensional, nonlinear data. While suitable for multi-input multi-output tasks, these models require substantial sample data and are prone to overfitting.[13]

Extreme learning machine (ELM) operates as a single-hidden layer feedforward network. The sole parameters requiring learning are the hidden-to-output weights. This char-

acteristic endows ELM with rapid training speeds and superior generalization performance.[14] Hidden layer parameters require no iterative adjustment. Output weights are calculated solely via the least squares method. Consequently, training speed surpasses that of back propagation neural network by one to two orders of magnitude.[15] In rare-earth material research, this facilitates the rapid screening of extensive candidate composition combinations.

Convolutional neural networks (CNNs) are deep learning (DL) models explicitly designed for processing data with grid-like topology.[16] CNNs extract local features through convolutional layers. They subsequently reduce dimensionality while retaining key features via pooling layers. Finally, fully connected layers perform classification or regression.[17] In materials science, CNNs analyze microstructural images to predict macroscopic performance.

2.2. Model based on decision tree

Decision tree regression (DTR) serves as the foundational algorithm, recursively partitioning the feature space into homogeneous subsets based on optimal splitting criteria until specific stopping conditions are met.[18] Its primary advantage lies in its intrinsic interpretability and visualization capabilities, allowing researchers to explicitly trace decision pathways. However, single decision trees are inherently prone to high variance and overfitting, particularly when processing datasets sensitive to noise or minor perturbations. To address these limitations, random forest regression (RF) leverages a bagging (bootstrap aggregating) strategy. Building upon this, gradient boosting decision tree (GBDT) and extreme gradient boosting (XGB) adopt a sequential boosting strategy to reduce bias. GBDT iteratively constructs weak learners to fit the negative gradient of the loss function from previous steps. XGB further optimizes this framework by incorporating a second-order Taylor expansion of the loss function and adding regularization terms to control model complexity. These modifications can improve optimization efficiency and help control model complexity and overfitting.

In the specific context of magnetostrictive material research, these ensemble learning methods offer a distinct advantage over DL by effectively mining patterns from small-sample datasets. They accurately model highly non-linear mappings between complex synthesis parameters — such as stoichiometry, annealing temperature, and orientation control — and key performance metrics like M_s and λ. Crucially, the feature importance mechanisms embedded in these algorithms provide a quantitative basis for physical interpretation. By identifying the relative contributions of specific rare-earth elements, interpretable ML can provide hypotheses regarding their possible roles in domain rotation and crystal-field-related effects, which require further physical validation. This transition from black-box prediction to interpretable analysis fundamentally transforms material design, shifting the paradigm from empirical trial-and-error to rational, data-driven optimization.

2.3. Other models for regression tasks

Support vector regression (SVR) represents the adaptation of support vector machines for regression tasks. Its primary objective is to define a function where deviations of all training samples remain within a preset threshold.[19] Simultaneously, it seeks to minimize model complexity. In predicting magnetostrictive properties, SVR effectively processes limited experimental data. It identifies the optimal hyperplane to facilitate accurate forecasting. The K-nearest neighbors (KNN) algorithm operates as a lazy learning model based on proximity similarity. It functions as a non-parametric, instance-based method suitable for both classification and regression. In regression contexts, KNN computes the distance between a new query instance and all training samples.[19] It subsequently selects the k nearest neighbors. The predicted value is typically derived as the average of these neighbors' target values. The KNN architecture is intuitively simple and requires no explicit training phase. However, its computational complexity escalates significantly with increasing data volume. In the exploration of magnetostrictive materials, KNN identifies analogues with similar compositions and processing histories. It subsequently predicts their potential magnetostrictive performance.

3. Magnetostrictive materials and devices

3.1. Rare earth-based magnetostrictive materials

Rare-earth GMMs are an important class of functional materials, owing to their strong magnetoelastic coupling between magnetic-field variation and structural deformation. This coupling makes them attractive for applications in spintronics, precision actuation, and energy harvesting. The earliest ML studies on rare-earth magnetostrictive materials mainly focused on composition–property prediction. The input data are typically structured numerical descriptors, such as alloy composition, magnetic field, heat-treatment parameters, and phase information, while the target outputs are macroscopic properties such as magnetostriction. For such tabular datasets with nonlinear relationships, traditional ML methods are particularly suitable. They can efficiently learn descriptor–property mappings without requiring explicit spatial representations. Liu *et al.*[20] addressed the non-linear correlation challenges associated with the magnetostriction of TbDyFe alloys. Ti content and external magnetic field were used as the input variables, while the magnetostriction coefficient was taken as the output. A three-layer BPNN was constructed to learn this low-dimensional nonlinear mapping. The coefficient of determination (R^2) can reach 0.991, and the absolute error of most data points is less than 5%. This study demonstrated that

BPNN can effectively address low-dimensional relationships when the dataset is relatively small but well targeted.

As the descriptor space expanded to multivariate experimental parameters, ensemble learning methods gradually became more advantageous. Hu *et al.*[21] developed a data-driven screening strategy for RFe$_2$-type GMMs, as shown in Fig. 1. The dataset integrated multiple descriptors, such as phase constitution, room-temperature magnetostriction (λ_a), heat-treatment conditions, and driving magnetic field. Among the tested models, XGB achieved the best predictive performance with an R^2 of 0.98, indicating excellent fitting ability and generalization. Based on this model, the magnetostriction distribution of $Tb_xDy_{1-x}Fe_yV_{2-y}$ alloys was mapped. As depicted in Fig. 2, the high-performance compositional regions were identified. Experimental validation showed that $Tb_{0.28}Dy_{0.72}Fe_{1.96}V_{0.04}$ reached a room-temperature magnetostriction of 1619.69 ppm under a low magnetic field of 12 kOe, outperforming many previously reported alloys.[22–26]

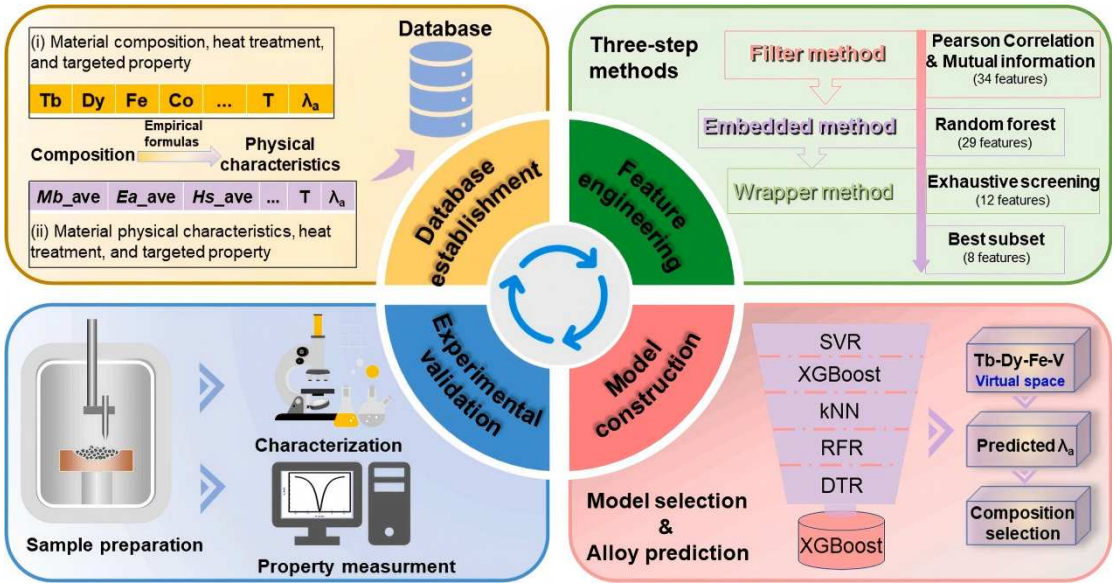


Fig. 1. Diagram of design strategy for RFe$_2$-type alloys with desired magnetostriction.[21]

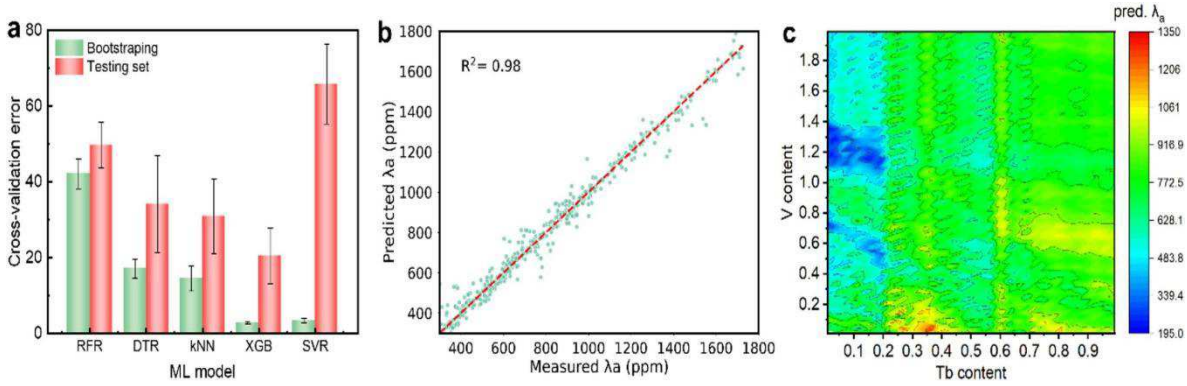


Fig. 2. Construction of machine learning model. (a) Cross-validation error of models obtained by bootstrapping resampling method through 100 iterations. (b) Comparison of the measured and predicted λ_a by XGB model for RFe$_2$-type compounds. (c) Predicted magnetostriction heatmap of Tb–Dy–Fe–V alloys.[21]

A similar conclusion was reached by Gong *et al.*,[27] who established a dual-stage framework to optimize the trade-off between magnetostriction and piezomagnetic properties in RFe$_2$. This approach combines ML prediction and high-throughput micromagnetic simulations (HTP-MMs). Using a dataset of 123 alloy compositions described by 18 elemental features, they compared DTR, SVR, RF, and gradient boosting regression trees (GBRT). DTR suffered from obvious overfitting, whereas SVR showed acceptable generalization but limited accuracy. RF improved robustness by reducing overfitting through randomization, but this also weakened the performance of individual weak learners. In contrast, GBRT achieved the best balance between accuracy and generalization, with R^2 values of 0.95 and 0.92 on the training and test sets. Simultaneously, it maintained low mean absolute errors (MAE) of 32.41 ppm and 99.02 ppm. The optimized GBRT model identified the high magnetostriction region in the $Tb_xDy_{1-x}Fe_y$ system. Compared with early BPNN-based models, these ensemble methods are more suitable for complex multicomponent alloy systems because they can bet-

ter handle higher-dimensional descriptor spaces and maintain predictive robustness. Therefore, traditional ML methods are preferred for composition–property prediction because the problem is usually formulated with structured descriptors and scalar property labels.

Although high prediction accuracy is valuable, composition–property prediction alone cannot fully support alloy design. Recent studies have increasingly emphasized interpretable alloy design, in which ML is used not only to predict properties but also to reveal feature contributions and support mechanism-guided optimization. In the work of Hu *et al.*,[21] Shapley additive explanations (SHAP) were further combined with the XGB model to quantify the contribution of individual descriptors to magnetostriction. As shown in Fig. 3(c), the SHAP summary plot, heatmap, and dependence plots revealed the relative influence of key variables such as average magnetic moment, bulk modulus, heat-treatment temperature, and compositional parameters. Moreover, the intersection of LOWESS fitting curves with SHAP = 0 was used to identify more precise descriptor thresholds. According to elasticity theory, bulk modulus correlates positively with Young's modulus, as described by

$$M_{\mathrm{b}} = \frac{M_{\mathrm{y}}}{3(1-\sigma)}, \tag{1}$$

where M_{b} and M_{y} denote bulk modulus and Young's modulus, respectively, and σ represents Poisson's ratio. This relationship provides additional physical context for the observed importance of $M_{\mathrm{b,ave}}$ in the ML model. Therefore, interpretable models are especially appropriate when the scientific objective is design guidance rather than prediction alone.

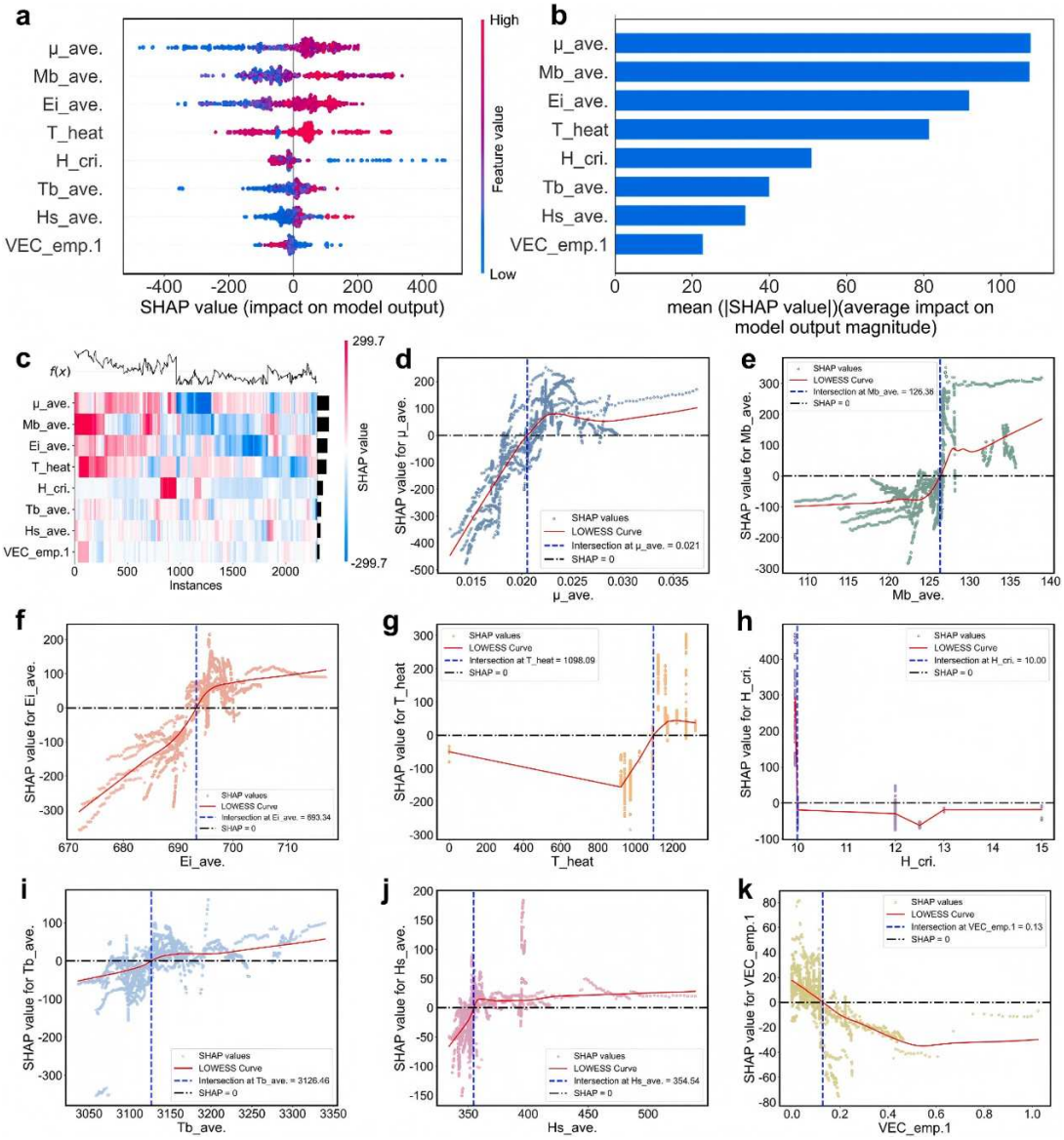


Fig. 3. (a) SHAP summary plot for each feature. The color intensity of each point stands for the impact of feature on the model prediction. (b) The ranking of feature contributions to λ_{a} based on SHAP. (c) Heatmap of global explanation using SHAP values. The SHAP value for key features: (d) μ_{ave}, (e) $\mathrm{Mb_{ave}}$, (f) $\mathrm{Ei_{ave}}$, (g) $\mathrm{T_{heat}}$, (h) $\mathrm{H_{cri}}$, (i) $\mathrm{Tb_{ave}}$, (j) $\mathrm{Hs_{ave}}$, (k) $\mathrm{VEC_{emp.1}}$, where the red solid line is the LOWESS fitted curve, the black dotted line represents SHAP = 0, and the blue dashed line denotes the intersection of the LOWESS curve and SHAP = 0.[21]

Since magnetostriction essentially stems from the lattice distortion caused by the magnetic-domain rotation and domain-wall motion, both of which are strongly influenced by microstructural factors such as grain orientation, grain size, grain boundary characteristics, and defect distribution, therefore, when the research objective shifts from component optimization to microstructure-performance mapping, models capable of preserving spatial connectivity become necessary. GNNs are particularly suitable for this purpose because a polycrystalline microstructure can be naturally represented as a graph. The grains correspond to nodes, and grain adjacency corresponds to edges. As shown in Fig. 4, Dai *et al.*[28] proposed a GNN framework for predicting the effective magnetostriction of polycrystalline $Tb_{0.3}Dy_{0.7}Fe_2$ alloys. In this model, the microstructure was represented as $G = (F, A)$. Here, A is the grain adjacency matrix, and F is the grain-feature matrix containing Euler angles, grain size, and the number of neighboring grains. The model captures intergranular interactions by integrating and updating message-passing layers:

$$F^{n+1} = \sigma\left(\hat{D}^{-\frac{1}{2}}\hat{A}\hat{D}^{-\frac{1}{2}}F^{n}W^{n}\right), \tag{2}$$

where σ is the ReLU activation function, $\hat{A}$ is the graph adjacency matrix, $\hat{D}$ is the degree diagonal matrix of $\hat{A}$, and $W^{(n)}$ is the trainable weight matrix. Message-passing operations were used to aggregate intergranular information and update node embeddings, allowing the model to learn how local grain features and neighborhood interactions jointly affect the macroscopic response. A fully connected layer subsequently combined the graph embedding with the external magnetic field H_x to predict the effective magnetostriction $\lambda_{xx}^{\mathrm{eff}}$. As shown in Fig. 4, the integrated gradients method was used to quantify the contribution of each physical feature of individual grains to magnetostriction. 492 three-dimensional polycrystalline microstructures containing 87981 grains were generated using Dream.3D. Phase-field simulations were then combined to obtain $\lambda_{xx}^{\mathrm{eff}}$ under varying external magnetic fields. GNN demonstrated exceptional performance in the prediction of magnetostriction for polycrystalline $Tb_{0.3}Dy_{0.7}Fe_2$ alloys. It achieved a MARE of only 8.24% on the test set, with the overall prediction error remaining within 12%. Therefore, GNN provides a unique advantage for describing grain connectivity and microstructure–property relationships that cannot be achieved using conventional ML models.

Table 2. Comparison of representative ML methods with respect to their research objectives.

Research objective	Representative algorithms	Advantages	Limitation
Composition–property prediction	BPNN, RF, XGB, GBDT	Structured numerical data with nonlinear relationships	Limited interpretability
Interpretable alloy design	SHAP + XGB	Quantify feature contributions and reveal physical mechanisms	High computational cost
Microstructure–property mapping	GNN	Capture grain connectivity and spatial interactions	High computational cost

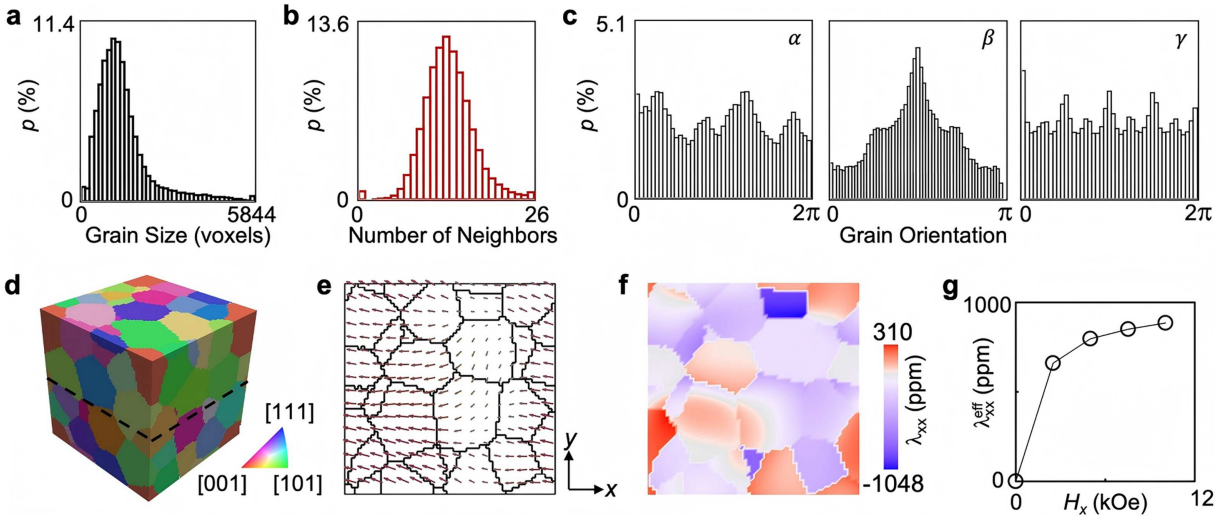


Fig. 4. Dataset of 3D polycrystalline microstructures and their effective magnetostriction. Distributions of (a) size (represented by the number of voxels), (b) the number of neighboring grains for a specific grain, and (c) three Euler angles of the 87981 grains in the entire dataset of 492 microstructures. (d) An example of 3D polycrystalline microstructure in the dataset (colored by grain orientation). (e) Local magnetization and (f) local magnetostriction λ_{xx} on the 2D slice shown in panel (d). (g) Effective magnetostriction of the 3D microstructure shown in panel (d) as a function of the applied field H_x.[28]

The aforementioned types of ML (listed in Table 2) address distinct scientific scenarios rather than competing directly with one another. Traditional ML algorithms, including BPNN, RF, XGB, and GBDT, are primarily designed for composition–property prediction using structured datasets. Interpretable ML frameworks, such as SHAP combined with XGB, are more valuable when researchers need to identify dominant factors and derive mechanism-relevant design rules.

In contrast, GNN extends ML to microstructure–property mapping by preserving grain connectivity and topological information. Therefore, the selection of ML methods should be determined by the research objective and data characteristics rather than algorithm complexity alone. This purpose-oriented perspective offers a clearer framework for selecting algorithms and understanding their respective roles in magnetostrictive materials research.

3.2. Iron-based magnetostrictive materials

Fe-based nanocrystalline soft magnetic materials are pivotal in high-frequency power electronics and precision sensing. Their near-zero λ is essential for achieving high permeability and low loss. The emergence of FINEMET materials in 1988 offered a novel pathway for material design. Their magnetostrictive behavior is strongly governed by nanoscale structural characteristics, such as grain size, crystalline phase fraction, and grain-boundary features. The λ of these materials is not a fixed constant. Instead, it is governed by nanocrystalline size, crystalline phase volume fraction, and residual stress. However, the strong coupling among composition, processing, and microstructure makes traditional trial-and-error development highly inefficient. In 2020, Wang *et al.*[29] accelerated the development of Fe-based soft magnetic alloys using ML models and random optimization frameworks. The original data were standardized according to atomic percentages, annealing temperature, and annealing time. Data cleaning, feature processing, and selection were carried out to obtain the final feature set. The primary objective was to maximize the saturation magnetic flux density B_s while minimizing the H_c, with simultaneous consideration of λ. This study systematically compared five algorithms, including linear regression, SVM, DTR, KNN, and RF. Figure 5 compares the predicted values of B_s, λ, and H_c against experimental data for all algorithms. The results showed that the most important features varied depending on the target property. The RF model achieved the best overall predictive performance. However, the RF generally has limited extrapolation capability beyond the range of the training data. Consequently, it is unable to identify the optimal component range or heat treatment window beyond the scope of the training data.

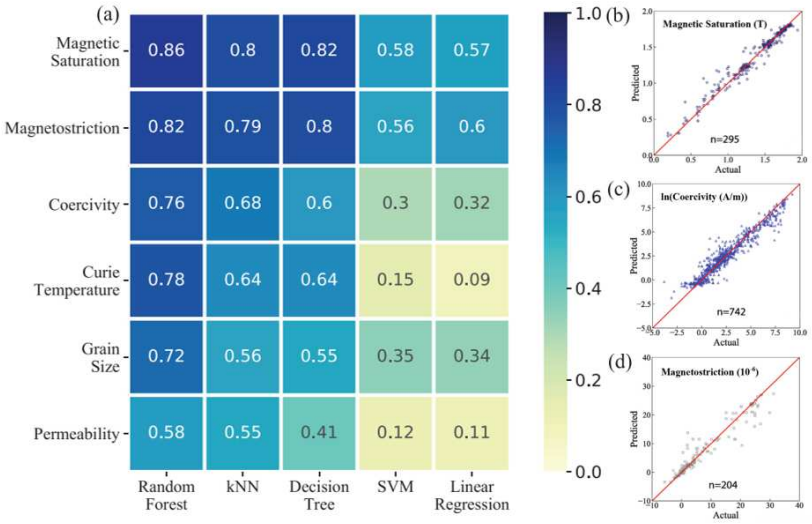


Fig. 5. (a) R^2 value of different machine learning algorithms. Comparison between predicted values from the machine learning model and experimental values for (b) magnetic saturation, (c) coercivity, and (d) magnetostriction.[29]

To further develop Fe-based soft magnetic materials combining low H_c, low loss, and high permeability, Tang *et al.*[30] focused on the synergistic optimization of magnetostriction coefficients and key magnetic properties in Fe-based amorphous/nanocrystalline alloys. This study integrated ML techniques into high-performance alloy design. It involved collecting 2417 sets of literature data to construct a comprehensive dataset covering properties such as λ, B_s, and H_c. The magnetostriction sub-dataset contained 233 material entries. Feature variables included 13 elemental compositions, annealing temperature, and annealing time. Figures 6(a) and 6(b) illustrate feature importance, highlighting distinct attributes critical for B_s and H_c, respectively. Results indicate that iron content and annealing temperature are the paramount attributes for B_s. Conversely, annealing temperature and the amorphous nature of the material are most critical for H_c. Beyond these primary factors, the significance of the remaining features declines gradually. Furthermore, feature importance analysis via the extreme gradient boosting (XGBT) model identified Fe content and annealing temperature as key determinants influencing λ. Notably, the regulatory effects of elemental and processing parameters on λ exhibit synergistic correlations with B_s and H_c. The predictive performance of four ML models — XGB, KNN, GB, and ANN — was evaluated using grid search and normalization methods, as shown in Fig. 6(c). Based on these analyses, the team designed a high-Fe con-

tent alloy: $Fe_{85}Si_2B_{8.5}P_{3.5}C_1$. Trace additions of P and C were employed to optimize glass-forming ability. This indirectly regulated magnetostriction levels. Consequently, the design achieved a synergistic enhancement of magnetostriction alongside B_s and H_c. The material simultaneously possesses high B_s, low H_c, and high T_c. The XGB model predicted magnetostriction values of 12.2 ppm and 10.4 ppm for the as-cast and annealed states of the $Fe_{85}Si_2B_{8.5}P_{3.5}C_1$ alloy, respectively. The deviation from experimental measurements (17.6 ppm and 15.5 ppm) was approximately 5 ppm. Although this deviation falls within a reasonable range, the model consistently underestimated the coefficients for both physical states. This systematic underestimation suggests deficiencies in the model's ability to capture the impact of phase transitions on magnetostrictive performance.

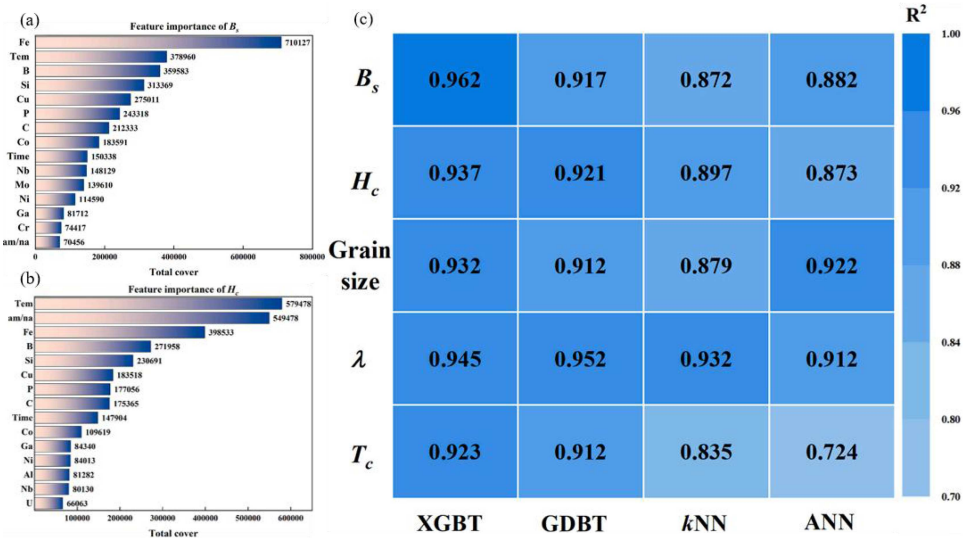


Fig. 6. Feature importance derived from the XGBT model for B_s (a) and H_c (b). (c) R^2 trending of XGBT, KNN, GBDT and ANN for predicting B_s, H_c, grain size, λ and T_c, respectively.[30]

The existing Jiles–Atherton (J–A) hysteresis model establishes a non-linear relationship between total magnetization (M) and applied magnetic field intensity (H). It achieves this by identifying five core characteristic parameters for ferromagnetic materials or composites via experimental measurement combined with algorithmic optimization. However, this standard model is inapplicable to magnetostrictive composites (MSCs). Consequently, Zhao *et al.*[31] proposed a technical route integrating a modified J–A model with data mining parameter identification. This approach realizes the prediction of magnetic properties for magnetostrictive materials. The traditional J–A model applies solely to single-phase ferromagnetic materials. It fails to account for factors such as the non-metallic matrix or particle shape orientation within MSCs. To address this, the study introduced a composite coefficient b:

$$b = \cos\theta \times V_f. \tag{3}$$

Here, θ represents the angle of the applied orientation field, and V_f denotes the volume fraction. Simultaneously, a demagnetization factor (N_d) was introduced to reconstruct core model parameters. This adaptation aligns the model with the hysteresis characteristics of MSCs. Hysteresis loop data for the $Tb_{0.25}Dy_{0.45}Ho_{0.31}Fe_{1.9}$ alloy were acquired using a vibrating sample magnetometer and a NIM-2000 magnetic testing system. Five categories of intermediate parameters were extracted. These parameters formed the raw dataset for identification. Subsequently, the differential evolution (DE) algorithm was employed as a data mining tool. It resolved the non-linear coupling issues among J–A model parameters. By defining an objective weight function — specifically minimizing the difference between simulated and experimental magnetization — the parameters were iteratively optimized. This process yielded an optimal parameter set adapted for MSCs. Using Tb–Dy–Ho–Fe alloy as the raw material and epoxy resin as the matrix, 1–3 type magnetostrictive composites were fabricated. Their major and minor hysteresis loops were subsequently tested. Following DE optimization, the modified J–A model simulation achieved a high degree of concordance with experimental data. This methodology allows for the prediction of MSC magnetic properties using only the original alloy data. It obviates the need for physical MSC fabrication and overcomes parameter deviations caused by direct equation solving.

3.3. Devices based on magnetostrictive materials

Magnetorheological (MR) foam represents a prototypical magnetic polymer composite. It is widely applicable in the development of flexible sensors and actuators for soft robotics. To realize the engineering deployment of MR foam-based devices, systematic modeling of their magnetostrictive behavior and mechanical properties is crucial. Addressing the challenge of predicting non-linear magnetostrictive performance, Rohim

et al.[32] pioneered the application of ELM and ANN in this domain. Their work provides a model for quantitatively predicting magnetostrictive properties based on composition and magnetic field conditions. This offers an efficient tool for the rapid design of MR foam devices in soft robotics. Initially, a rheometer was utilized to test the magnetostrictive performance of five MR foam variants under magnetic fields ranging from 0 to 0.78479 T. A raw dataset was constructed based on these experimental results. Following data cleaning and normalization, the model architecture was designed using a single hidden layer feedforward network framework. Upon completion of training, the R^2 and root mean square error (RMSE) were adopted as evaluation metrics. These quantitatively characterized the predictive accuracy of the models. The ELM series models significantly outperformed traditional ANN models in stress prediction. Specifically, the ELM model utilizing the hard limit activation function exhibited optimal performance. Its strain prediction achieved an R^2 of 0.999 and an RMSE below 0.003. Furthermore, no overfitting was observed across test samples with varying carbonyl iron powder contents. These results indicate that the ELM model can effectively reproduce the observed relationship between the input variables and the measured magnetostrictive response. However, ML models like ELM are intrinsically black box systems. While they achieve high-precision prediction, they fail to clearly elucidate the internal physical mechanisms linking magnetic fields, microstructure, and magnetostrictive behavior. This opacity limits their in-depth application in innovative material development.

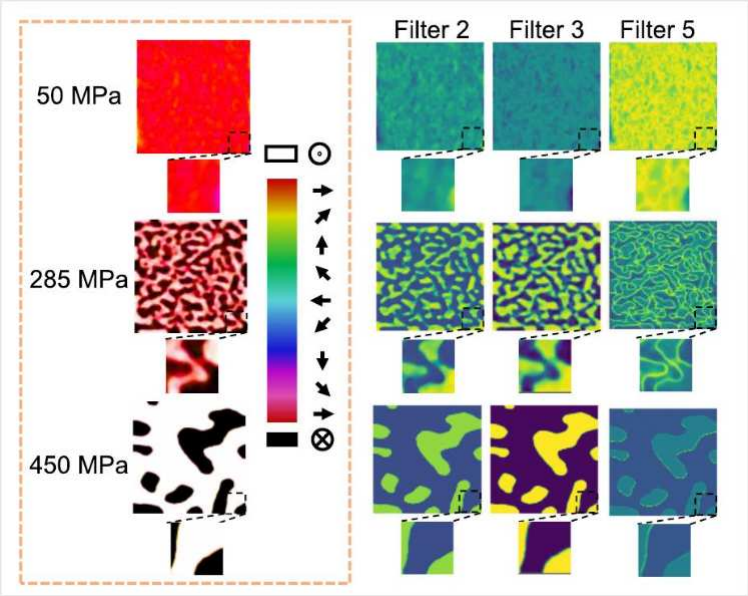


Fig. 7. Magnetic domains of $Tb_{0.27}Dy_{0.73}Fe_2$ under different stresses and the corresponding feature maps.[33]

The high magneto-elastic alloy, as the core sensing element, can meet the requirements for high-precision micro-strain/stress detection. Gong *et al.*[33] integrated DL with the magnetic domain response characteristics of magnetostrictive materials $Tb_{0.27}Dy_{0.73}Fe_2$. It achieved precise detection of micro-strains at the micrometer scale. Initially, micromagnetic simulations established a polycrystalline $Tb_{0.27}Dy_{0.73}Fe_2$ thin film model. Tensile stresses ranging from 0 to 500 MPa and reverse unloading processes were applied. This generated images of stress-driven magnetic domain evolution. A total of 501 magnetic domain images under varying stresses were partitioned into training, validation, and test sets. The ratio was maintained at 3:1:1. These images encapsulate stress-sensitive features such as magnetic moment reorientation and domain wall migration. Thus, they provide high-quality sample support for DL. Regarding model construction, a CNN architecture was adopted. It comprises two convolutional layers, two max-pooling layers, and a fully connected layer with 256 neurons. ReLU was employed as the activation function to mitigate gradient vanishing. Additionally, the Adam algorithm with adaptive learning rate served as the optimizer. Mean squared error (MSE) was selected as the loss function. Following 996 iterations of optimization, the model yielded a mean absolute error (MAE) of 1.35 MPa for the training set. The test set achieved an MAE of 2.10 MPa. The model demonstrates excellent generalization capabilities, particularly within the low-stress range of 0–200 MPa. It precisely captures strain variations on the order of 1.25×10^{-5} with a prediction error of merely 0.37 MPa. Consequently, the detection resolution far surpasses traditional x-ray techniques.[34] Figure 7 displays the magnetic domains and corresponding feature maps of $Tb_{0.27}Dy_{0.73}Fe_2$ under varying stresses. This confirms the model's ability to automatically extract key domain features. Filter 3 focuses on identifying vertical mag-

netic domain stripes. Meanwhile, filter 5 precisely captures domain wall contours. The synergistic action of multiple filters integrates microscopic details such as magnetic moment direction and domain size. This provides a clear physical basis for stress/strain quantization. The research transforms the magnetic domain response into image features recognizable by DL. It establishes a quantitative correlation between microscopic magnetic structure and macroscopic stress/strain. However, current validation relies solely on a single polycrystalline thin film model. It does not account for the impact of compositional fluctuations or temperature variations on detection accuracy.

4. Prospects

4.1. Data scarcity and quality dilemma

The effectiveness of ML and DL in the field of rare earth functional materials is fundamentally constrained by the scarcity of high-quality, standardized datasets. First, the acquisition of high-fidelity experimental data is inherently prohibitively expensive and suffers from significant temporal latency. The currently available datasets only contain a few hundred sample points, which is far less than the massive repositories required to train robust deep neural networks.[35] Second, the data distribution exhibits severe structural bias and sparsity within the high-dimensional compositional space. Previous studies have overly focused on a few mature and high-performance systems, such as the Terfenol-D and Galfenol series. In contrast, a large number of exploratory areas, especially those involving novel transition metal doping or light rare earth substitution, still lack sufficient supervisory signals.[36] Third, data heterogeneity presents an intractable obstacle to model convergence. Significant discrepancies exist in fabrication protocols and testing standards across different research groups. This inconsistency is regarded as a confounding variable. If not strictly handled, it may introduce non-physical illusions into the model and obscure intrinsic structure–property relationships.

One promising strategy for addressing data scarcity is transfer learning.[37] Transfer learning can transfer knowledge from data-rich related magnetic material systems. Representative source domains include permanent magnets, soft magnetic alloys, magnetic refrigeration materials, and magnetic thin films. These materials share common descriptors, such as elemental composition, magnetic moments, crystal structures, and thermodynamic parameters. Pretrained models developed from these datasets can provide transferable feature representations, thereby reducing the amount of task-specific data required for magnetostrictive materials. Another promising direction is to establish multimodal datasets so that machine learning models can learn physically meaningful feature representations rather than relying solely on statistical correlations.[38] In addition, active learning provides another effective strategy for improving dataset quality. Instead of randomly selecting new experiments, the model actively identifies compositions with the highest uncertainty and recommends them for experimental validation. Newly acquired data are subsequently incorporated into the training dataset, allowing continuous model refinement.[39] Such closed-loop optimization significantly reduces experimental costs while accelerating the discovery of high-performance magnetostrictive materials. Transfer learning, multimodal data fusion, and active learning are expected to become key technologies for overcoming the limitations of current small-data scenarios in magnetostrictive materials

4.2. Interpretability deficit

Despite the predictive prowess of current ML models, their inherent black-box nature constitutes a critical bottleneck hindering widespread adoption in closed-loop material design. The mutual conversion of magnetic and elastic energy is driven by intricate mechanisms ranging from 4f electron shell interactions and spin–orbit coupling to irreversible magnetic domain wall motion under stress fields. However, mainstream algorithms remain fundamentally statistical. They capture local correlations within labeled data but lack the capacity to comprehend these underlying physical principles. Although the physically interpretable framework proposed by Hu *et al.*[21] significantly improves the understanding of feature contributions, its interpretability is still derived from the internal behavior of the ML model rather than from explicit physical equations. Consequently, the feature importance depends strongly on the selected prediction model and training dataset. The model accuracy degrades sharply when extrapolating to unknown chemical spaces or novel crystal structures.[40] This inability to generalize beyond the training distribution severely impedes cross-system material discovery.

More importantly, current interpretable ML models mainly establish statistical correlations between descriptors and target properties. Several key physical mechanisms governing magnetostriction are still not explicitly incorporated into existing learning frameworks. For example, the magnetoelastic coupling between magnetic moments and lattice strain, the magnetic domain nucleation and domain-wall motion, the crystal-field interactions of rare-earth atoms, phase transformation during processing, and the thermodynamic evolution under different heat treatment conditions are not considered. As a result, current models provide feature attribution but cannot fully reveal the physical origin of magnetostrictive behavior.

In this context, physics-informed neural networks (PINNs) may provide a promising solution for integrating multi-physics mechanisms into ML models.[41] Unlike purely data-driven models, PINNs incorporate governing equations,

boundary conditions, and prior physical knowledge directly into the training process. By constraining model predictions to satisfy known physical laws, PINNs can potentially improve physical consistency, interpretability, and generalization. For magnetostrictive materials, constitutive relations describing magnetoelastic coupling, thermodynamic equilibrium, and phase evolution could, in principle, be embedded into such learning frameworks. Nevertheless, the application of PINNs to magnetostrictive materials still faces several important challenges. First, magnetostriction is governed by strongly coupled processes involving magnetic, mechanical, thermal, and microstructural evolution. The formulation of appropriate governing equations is highly nontrivial. Second, some key mechanisms, such as domain-wall motion, phase transformation, and processing-induced microstructural evolution, are difficult to describe accurately in a unified PINN framework. Third, the successful training of PINNs often requires carefully designed physical constraints, numerical stability, and sufficient high-quality data for validation. Therefore, the effective application of PINNs in this field still requires further methodological development and system-specific adaptation.

4.3. Cross-scale coupling challenge

Although magnetostriction is inherently governed by strongly coupled processes across electronic, microstructural, and macroscopic scales, current ML studies have not yet fully realized genuine cross-scale information fusion.[42] Most existing studies still remain confined to isolated scales. Ensemble learning models are primarily used to describe composition–property relationships. GNN models are mainly developed for microstructure–property prediction, and DL models are usually applied to image recognition or device applications. Although these models often achieve high predictive accuracy within their respective domains, they are generally developed independently. Information across different physical scales is rarely integrated within a unified framework.[43] One major challenge lies in the heterogeneity of multiscale data, as descriptors derived from first-principles calculations, microstructural images, and experimental property measurements differ substantially in physical meaning, spatial resolution, and representation format. Another key limitation is the discontinuity of the physical-information pathway. Most existing models directly establish statistical correlations between input variables and target properties, while the intermediate mechanisms linking electronic interactions, domain evolution, microstructure formation, and macroscopic response are often ignored. In addition, the imbalance of available datasets at electronic, microstructural, and macroscopic levels further hinders joint training and robust generalization. To address these issues, future research should focus on developing physics-informed multimodal frameworks capable of integrating heterogeneous data, hierarchical learning architectures that explicitly model information transfer across scales, and knowledge-guided representations that preserve the causal relationships among composition, electronic structure, microstructure, and functional properties. Such efforts may provide a practical route toward genuine cross-scale coupling and more reliable intelligent design of magnetostrictive materials.

4.4. Critical supply chain bottlenecks

The transition of rare-earth magnetostrictive materials from laboratory prototypes to industrial commodities faces severe bottlenecks beyond mere technical performance. The primary constraint lies in the supply chain ecosystem, where the core heavy rare-earth elements are highly susceptible to geopolitical dynamics and trade policy shifts.[44] This fragility manifests as persistent price volatility, significantly escalating fabrication costs and raising barriers to market entry. However, existing models predominantly maximize physical attributes, such as magnetostriction and magnetic stability, while treating cost and environmental impact as secondary externalities. They lack integrated mechanisms for cost risk management and comprehensive life cycle assessment, effectively blinding researchers to the hidden costs of supply interruptions and the carbon footprint of extraction and purification processes. In the context of intensifying global resource competition and the drive for green development, this single-objective focus is obsolete. There is an urgent strategic imperative to develop multi-objective optimization frameworks capable of navigating the complex trade-offs between performance, cost, and sustainability. Such frameworks are essential for guiding the discovery of alloys with reduced heavy rare-earth content or doping-modified alternatives. Ultimately, achieving a synergistic balance among functional properties, supply security, and eco-friendliness is the critical step toward realizing robust, sustainable industrialization.

Acknowledgments

Project supported by the National Key Research and Development Program of China (Grant No. 2023YFA1610400), the Beijing Natural Science Foundation (Grant No. JR26007), the National Natural Science Foundation of China (Grant Nos. 52371169 and U25A6010), the National Key Research and Development Program of China (Grant Nos. 2021YFB3501202 and 2022YFB3505201), and the Advanced Materials-National Science and Technology Major Project (Grant No. 2025ZD0618203).

References

[1] Tang Y M, Xu X L, Huang Y, Tang Z X and Tang S L 2017 *Chin. Phys. B* **26** 127502

[2] Murtaza A, Yang S, Zhou C and Song X P 2016 *Chin. Phys. B* **25** 096107
[3] Karafi M R and Poursadr M 2024 *J. Magn. Magn. Mater.* **611** 172636
[4] Huhe B, Yibole H, Guillou F, Dijk N H and Brück E 2026 *APL Mater.* **14** 011107
[5] Amon A, Baker A A, Shittu J, Moore E E, Kim E, Rietema C, Henderson H B, Abeykoon A M M and McCall S K 2023 *J. Magn. Magn. Mater.* **586** 171214
[6] Liu D, Li Y, Sun R X, Qi X and Shen B G 2025 *Acta Phys. Sin.* **74** 137102 (in Chinese)
[7] Ponomarova S, Ponomarov O and Koval Y 2025 *J. Magn. Magn. Mater.* **634** 173551
[8] Agada J O, McAninch A, Day H, Tanyu Y, McCombs E, Koohpayeh S M, Toby B H, Wang Y S and Biswas A 2026 *APL Mach. Learn.* **4** 026113
[9] Wei P, Bai H, Liu Y, Zhuang L, Yu H L and Chu Y H 2025 *J. Materiomics* **11** 100967
[10] Chen J, Liu J, Zhang M J, Dong Z Y, Peng Z J, Ji X Y, Liu M, Zhang L T, Zhang A Q and Zhu H 2023 *J. Mater. Chem. A* **11** 8988
[11] Lei S J, Bai D, Ren Z Z and Lyu M J 2021 *Chin. Phys. Lett.* **38** 051101
[12] Zhu Q J, Tian L C, Yang X H, Gan L F, Zhao N and Ma Y Y 2014 *Chin. Phys. Lett.* **31** 072901
[13] Lazzus J A 2011 *Chin. Phys. Lett.* **28** 110504
[14] Omkari D Y and Shaik K 2026 *AIP Conf. Proc.* **3284** 070019
[15] Hao S Q, Singh P, Smirnov A V, Johnson D D, Alman D E and Gao M C 2025 *J. Appl. Phys.* **138** 085103
[16] Xu F J, Zhang Y, Liu Q, Li T, Lan M Y and Zhang Y T 2024 *Rev. Sci. Instrum.* **95** 105117
[17] Chen Y 2026 *Chin. Phys. Lett.* **43** 060001
[18] Gu Y H, Zhao N J, Ma M J, Meng D S, Yu Y, Jia Y, Fang L, Liu J G and Liu W Q 2016 *Chin. Phys. Lett.* **33** 085201
[19] Fazizadeh S and Maedanqom H N 2025 *APL Mach. Learn.* **3** 046111
[20] Liu H and Huang K N 2013 *Hot Work. Technol.* **42** 63
[21] Hu P Q, Zhou C, Zhang R S, Ding S D, Guo Y J, Wang B, Xue D Z, Ma Y Z, Dai Z Y, Zhang Y, Tian F H and Yang S 2025 *Mater. Des.* **252** 113799
[22] Chin T S, Chen F M and Fang J S 1997 *IEEE Trans. Magn.* **33** 3946
[23] Liu Y, Zhao T L, Ju W W and Shi S Q 2017 *J. Materiomics* **3** 159
[24] Yuan R H, Liu Z, Balachandran P V, Xue D Q, Zhou Y M, Ding X D, Sun J, Xue D Z and Lookman T 2018 *Adv. Mater.* **30** 1702884
[25] Vergara J R and Estévez P A 2014 *Neural Comput. Appl.* **24** 175
[26] Wang F J and Zhang Y 2008 *Mater. Sci. Eng. A* **496** 214
[27] Gong J H, Zhang Z M, Zhang C L, Hu P Q, Zhou C, Wang D H and Yang S 2024 *Rare Met.* **43** 2251
[28] Dai M Y, Demirel M F, Liang Y Y and Hu J M 2021 *npj Comput. Mater.* **7** 103
[29] Wang Y H, Tian Y F, Kirk T, Laris O, Ross J H, Noebe R D, Keylin V and Arróyave R 2020 *Acta Mater.* **194** 144
[30] Tang S D, Sun R, He Y F, Liu G C, Wang R X, Liu Y Q and Tang C Y 2024 *Mater. Des.* **248** 113461
[31] Zhao R and Wang B W 2018 *J. Intell. Fuzzy Syst.* **35** 461
[32] Rohim M A S, Nazmi N, Bahiuddin I, Mazlan S A, Norhaniza R, Yamamoto S I, Nordin N A and Aziz S A A 2022 *J. Appl. Polym. Sci.* **139** 52798
[33] Gong J H, Zhang Z M, Wang H C and Wang D H 2024 *IEEE Sens. J.* **24** 4350
[34] Gómez J F and Albrecht H L 2026 *Phys. Lett. A* **593** 132018
[35] Liu Y, Yang Z W, Zou X X, Ma S C, Liu D H, Avdeev M and Shi S Q 2023 *Natl Sci. Rev.* **10** nwad125
[36] Hakami A 2024 *Sci. Rep.* **14** 9645
[37] Kong J G, Li Q X, Li J, Liu Y and Zhu J J 2022 *Chin. Phys. Lett.* **39** 9
[38] Huang T L, He Y F, Jiang H and Zhang J Z 2025 *Phys. Fluids* **37** 086161
[39] Wu Y D, Meng Z M, Wen K, Mi C D, Zhang J and Zhai H 2020 *Chin. Phys. Lett.* **37** 103201
[40] Jain A 2024 *Curr. Opin. Solid State Mater. Sci.* **33** 101189
[41] Zhou H J and Chen Y 2026 *Chin. Phys. Lett.* **43** 040003
[42] Yu S S, Liu J B and Xiong H 2025 *Chin. Phys. B* **34** 068502
[43] Feng S H, Chen H F, Zhang J, An M and Zhang G 2026 *Chin. Phys. Lett.* **43** 020801
[44] Cui H J, Wang F, Ma C, Zhang H J and Liu K 2024 *Sci. China Mater.* **67** 2376